Bistability and Low-Energy Electron Transfer in Cobalt Complexes Containing Catecholate and Semiquinone Ligands

Ok-Sang Jung[†] and Cortlandt G. Pierpont[*]

Department of Chemistry and Biochemistry, University of Colorado, Boulder, Colorado 80309

Received October 6, 1993[⊗]

Studies have been carried out on intramolecular cobalt–quinone electron transfer for a series of complexes of general form Co^{III}(N–N)(SQ)(Cat), where N–N is 2,2′-bipyridine (bpy), *N,N,N′,N′*-tetramethylethylenediamine (tmeda), 1,10-phenanthroline (phen), bis(2-pyridyl) ketone $(py)_2CO$, 5-nitro-1,10-phenanthroline (NO_2phen), dipyrido[3,2-*a*:2′,3′-*c*]phenazine (dppz), and 4,5-diazafluoren-9-one (dafl) and SQ and Cat are the 3,5- or 3,6-di-*tert*-butylcatechol and semiquinone ligands. Optical absorptions that appear in the 2500-nm (4000-cm^{-1}) region of the infrared for the Co(III) complexes are assigned as Cat → Co(III) charge transfer transitions. Spectral changes observed for the complexes in toluene solution result from an equilibrium between Co^{III}(N–N)(SQ)(Cat) and Co^{II}(N–N)$(SQ)_2$ redox isomers. Magnetic measurements on solid samples of Co(bpy)(3,5-DBSQ)(3,5-DBCat) and Co(phen)(3,6-DBSQ)(3,6-DBCat) show that the equilibrium exists in the solid state. The temperature range of the equilibrium is dependent upon the donation effect of the nitrogen coligand; values for the Co(III)/Co(II) transition temperature have been determined that follow coligand donor strength. Crystallographic characterization of Co(tmeda)(3,6-DBSQ)(3,6-DBCat) (Co(tmeda)(3,6-DBSQ)(3,6-DBCat): monoclinic, $P2_1/n$, a = 11.379(2) Å, *b* = 34.510(5) Å, *c* = 17.583(3) Å, β = 91.73(1)°, V = 6902(2) Å^3, *Z* = 8) has provided bond lengths showing that the metal is low-spin Co(III) at room temperature. Structural characterization of $Co(NO_2phen)(3,6\text{-}DBSQ)_2$ ($Co(NO_2phen)(3,6\text{-}DBSQ)_2$·2toluene: monoclinic, *Pc*, *a* = 12.626(2) Å, *b* = 11.297(2) Å, *c* = 17.974(3) Å, β = 105.55(1)°, *V* = 2470(1) Å^3, *Z* = 2) and Co(dafl)$(3,6\text{-}DBSQ)_2$ (Co(dafl)$(3,6\text{-}DBSQ)_2$·2toluene: monoclinic, *Pc*, *a* = 12.385(5) Å, *b* = 11.230(5) Å, *c* = 17.892(6) Å, β = 105.41(2)°, *V* = 2400(2) Å^3, *Z* = 2) has shown that the complex molecules are trigonal prismatic in structure at room temperature, with features that are consistent with the high-spin Co(II) charge distribution. Magnetic measurements on $Co(NO_2phen)(3,6\text{-}DBSQ)_2$ indicate that it remains in the Co(II) form at low temperature.

Introduction

Several years ago, we reported that a complex of cobalt-containing quinone ligands exhibited facile metal–quinone electron transfer in solution.[1] The complex was found to exist in a Co(III) form, Co^{III}(bpy)(3,5-DBSQ)(3,5-DBCat), in the solid state at room temperature. In toluene solution an equilibrium between Co(III) and Co(II) species (eq 1)was observed from changes in

$$Co^{III}(bpy)(3,5\text{-}DBSQ)(3,5\text{-}DBCat) \rightleftarrows Co^{II}(bpy)(3,5\text{-}DBSQ)_2 \quad (1)$$

magnetism and magnetic resonance spectra. Tautomeric forms of the complex are related by the transfer of an electron between the metal and a chelated quinone ligand. Recent studies on the magnetic properties of related cobalt complexes have shown that the electron transfer process may be observed on samples in the solid state.[2,3] It has since been reported for complexes of other metals containing quinone ligands,[4] and it appears responsible for unique thermo- and photophysical properties of certain concatenated metal–quinone complexes in the solid state.[2,5] Intramolecular electron transfer is a consequence of charge localization within the molecule and the close energy separation between localized quinone and metal electronic levels. It is reasonable to expect that molecules that show this property should have associated optical transitions, but at unusually low energies. We now report the results of studies on tautomeric equilibria for a series of cobalt complexes prepared with nitrogen-donor coligands of varying strength as σ-donors. Ligands used in this investigation include 2,2′-bipyridine (bpy), *N,N,N′,N′*-tetramethylethylenediamine (tmeda), 1,10-phenanthroline (phen), bis(2-pyridyl) ketone ($(py)_2CO$), 5-nitro-1,10-phenanthroline (NO_2phen), dipyrido[3,2-*a*:2′,3′-*c*]phenazine (dppz), and 4,5-diazafluoren-9-one (dafl). The results of this investigation show that

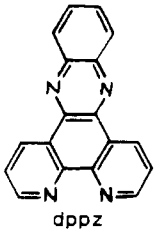

dppz

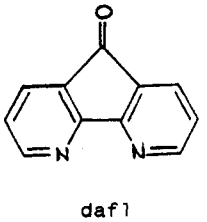

dafl

the Co^{III}(N–N)(SQ)(Cat) forms of the complexes have intense Cat → Co(III) charge transfer transitions in the 2500-nm region of the infrared. Tautomeric equilibria have been studied in solution and in the solid state. Transition temperatures (T_c) for the Co(III)/Co(II) equilibria in both media have been found to be dependent upon the coligand.

[†] Permanent address: Korea Institute of Science and Technology, Cheongryang, Seoul, Korea.

[⊗] Abstract published in *Advance ACS Abstracts,* April 1, 1994.

(1) Buchanan, R. M.; Pierpont, C. G. *J. Am. Chem. Soc.* **1980**, *102*, 4951.
(2) Abakumov, G. A.; Cherkasov, V. K.; Bubnov, M. P.; Ellert, O. G.; Dobrokhotova, Z. B.; Zakharov, L. N.; Struchkov, Y. T. *Dokl. Akad. Nauk* **1993**, *328*, 12.
(3) (a) Adams, D. M.; Dei, A.; Rheingold, A. L.; Hendrickson, D. N. *Angew. Chem., Int. Ed. Engl.* **1993**, *32*, 880. (b) Adams, D. M.; Dei, A.; Rheingold, A. L.; Hendrickson, D. N. *J. Am. Chem. Soc.* **1993**, *115*, 8221.
(4) (a) Lynch, M. W.; Hendrickson, D. N.; Fitzgerald, B. J.; Pierpont, C. G. *J. Am. Chem. Soc.* **1984**, *106*, 2041. (b) Abakumov, G. A.; Razuvaev, G. A.; Nevodchikov, V. I.; Cherkasov, V. K. *J. Organomet. Chem.* **1988**, *341*, 485. (c) Rakhimov, R. R.; Solozhenkin, P. M.; Kopitaya, N. N.; Pupkov, V. S.; Prokof'ev, A. I. *Dokl. Akad. Nauk SSSR* **1988**, *300*, 1177. (d) Abakumov, G. A.; Garnov, V. A.; Nevodchikov, V. I.; Cherkasov, V. K. *Dokl. Akad. Nauk SSSR* **1989**, *304*, 107.
(5) Lange, C. W.; Foldeaki, M.; Nevodchikov, V. I.; Cherkasov, V. K.; Abakumov, G. A.; Pierpont, C. G. *J. Am. Chem. Soc.* **1992**, *114*, 4220.

0020-1669/94/1333-2227$04.50/0

Table 1. Crystallographic Data for Co(tmeda)(3,6-DBSQ)(3,6-DBCat), $Co(NO_2phen)(3,6\text{-}DBSQ)_2 \cdot 2C_7H_8$, and $Co(dafl)(3,6\text{-}DBSQ)_2 \cdot 2C_7H_8$[a]

	Co(tmeda)(3,6-DBSQ)(3,6-DBCat)	$Co(NO_2phen)(3,6\text{-}DBSQ)_2 \cdot 2C_7H_8$	$Co(dafl)(3,6\text{-}DBSQ)_2 \cdot 2C_7H_8$
mol wt	615.8	892.9	864.0
color	blue-green	black-brown	black
crystal system	monoclinic	monoclinic	monoclinic
space group	$P2_1/n$	Pc	Pc
a, Å	11.379(2)	12.626(2)	12.385(5)
b, Å	34.510(5)	11.297(2)	11.230(5)
c, Å	17.583(3)	17.974(3)	17.892(6)
β, deg	91.73(1)	105.55(1)	105.41(2)
vol, Å^3	6902(2)	2470(1)	2400(2)
Z	8	2	2
D_{calc}, g cm^{-3}	1.185	1.201	1.196
μ, mm^{-1}	0.530	0.393	0.401
R, R_w	0.058, 0.062	0.054, 0.064	0.061, 0.061
GOF	1.14	1.30	1.29

[a] Radiation, Mo Kα (0.710 73 Å); temp, 293–298 K. $R = \Sigma||F_o| - |F_c||/\Sigma|F_o|$. $R_w = [\Sigma w(|F_o| - |F_c|)^2/\Sigma w(F_o)^2]^{1/2}$

Experimental Section

Materials. 3,5-Di-*tert*-butyl-1,2-benzoquinone (3,5-DBBQ), 2,2′-bipyridine (bpy), *N,N,N′,N′*-tetramethylethylenediamine (tmeda), 1,-10-phenanthroline (phen), 5-nitro-1,10-phenanthroline (NO_2phen), and bis(2-pyridyl) ketone ($(py)_2CO$) were purchased from Aldrich. Dicobaltoctacarbonyl was purchased from Strem Chemical Co. 3,6-Di-*tert*-butyl-1,2-benzoquinone (3,6-DBBQ),[6a] dipyrido[3,2-*a*:2′,3′-*c*]phenazine (dppz),[6b] 4,5-diazafluoren-9-one (dafl)[6c] and Co(bpy)(3,5-DBSQ) (3,5-DBCat)[1] were prepared using literature procedures. An initial sample of Co(bpy)(3,6-DBSQ)(3,6-DBCat) was provided by Professor G. A. Abakumov.[2]

Complex Syntheses. Co(tmeda)(3,6-DBSQ)(3,6-DBCat). $Co_2(CO)_8$ (86 mg, 0.25 mmol) and tmeda (60 mg, 0.52 mmol) were combined in 30 mL of toluene. The mixture was stirred for 5 min, and 3,6-DBBQ (220 mg, 1.0 mmol) in 30 mL of toluene was added. The solution was stirred under Ar for 2 h at room temperature. Evaporation of the solvent produced a dark blue residue of the complex. Crystals of Co(tmeda)-(3,6-DBSQ)(3,6-DBCat) suitable for crystallographic characterization were grown from acetone solution. Yield: 234 mg (76%).

Synthetic procedures used to form complexes containing other nitrogen-donor ligands followed the procedure above. Details are included with the supplementary material.

Physical Measurements. Electronic spectra were recorded on a Perkin-Elmer Lambda 9 spectrophotometer equipped with a RMC-Cryosystems cryostat. Magnetic measurements were made using a Quantum Design SQUID Magnetometer at a field strength of 5 kG. Infrared spectra were recorded on a Perkin-Elmer 1600 FTIR with samples prepared as KBr pellets. EPR spectra were recorded on a Bruker ESP-300E and referenced to DPPH as the g-value standard.

Crystallographic Structure Determinations. Co(tmeda)(3,6-DBSQ)-(3,6-DBCat). Dark blue crystals of the complex were grown from acetone. Axial photographs indicated monoclinic symmetry and the centered settings of 25 intense reflections with 2θ values between 20° and 25° gave the unit cell dimensions listed in Table 1. Data were collected by θ–2θ scans within the angular range 3.0–45°. Density measurements together with the unit cell volume indicated that there were two independent complex molecules per asymmetric region of the unit cell. Both Co atoms were located on a sharpened Patterson map and phases generated from the locations of these atoms gave the positions of other atoms of the structure. Final cycles of refinement converged with discrepancy indices of $R = 0.058$ and $R_w = 0.062$. Selected atom positions are listed in Table 2; tables containing a full listing of atom positions, anisotropic displacement parameters, and hydrogen atom locations are available as supplementary material.

$Co(NO_2phen)(3,6\text{-}DBSQ)_2$. Black-brown crystals of the complex were grown from toluene. Axial photographs indicated monoclinic symmetry and the centered settings of 25 intense reflections with 2θ values between 21 and 35° gave the unit cell dimensions listed in Table 1. Data were collected by θ–2θ scans within the angular range 3.0–50°. Density measurements together with the unit cell volume indicated that there were two complex molecules per unit cell. The coordinates of the coblt atom were determined using a sharpened Patterson map, and phases generated from the location of this atom gave the positions of other atoms of the structure including the locations of two toluene solvent molecules of crystallization. Final cycles of refinement converged with discrepancy indices of $R = 0.054$ and $R_w = 0.064$. Selected atom locations are listed in Table 3; tables containing a full listing of atom positions, anisotropic displacement parameters, and hydrogen atom locations were deposited with an earlier communication of this structure.[7]

Table 2. Selected Atom Coordinates (×10^4) and Equivalent Isotropic Displacement Parameters (Å^2) for Co(tmeda)(3,6-DBSQ)(3,6-DBCat)

	x/a	y/b	z/c	U(eq)
Co1	1621(1)	2312(1)	4312(1)	42(1)
O1	415(4)	2673(1)	4406(2)	44(2)
O2	2638(4)	2748(1)	4333(3)	45(2)
C1	834(6)	2998(2)	4678(3)	37(3)
C2	109(6)	3300(2)	4961(4)	42(3)
C3	718(7)	3618(2)	5219(4)	47(3)
C4	1943(7)	3653(2)	5198(4)	49(3)
C5	2675(6)	3378(2)	4908(4)	43(3)
C6	2085(6)	3041(2)	4637(3)	37(3)
O3	1810(4)	2292(1)	5360(2)	43(2)
O4	506(4)	1916(1)	4406(3)	45(2)
C15	866(6)	2116(2)	5647(4)	36(3)
C16	652(6)	2138(2)	6427(4)	38(3)
C17	−379(6)	1956(2)	6644(4)	46(3)
C18	−1121(6)	1767(2)	6129(4)	46(3)
C19	−893(6)	1742(2)	5346(4)	38(3)
C20	136(7)	1919(2)	5123(4)	44(3)
N1	1471(6)	2319(2)	3158(3)	54(2)
N2	2940(5)	1928(2)	4197(3)	57(3)
Co2	2801(1)	5310(1)	8113(1)	46(1)
O5	1443(4)	5623(1)	7959(3)	49(2)
O6	2866(4)	5298(1)	7056(2)	45(2)
C35	1066(6)	5594(2)	7256(4)	39(3)
C36	−25(6)	5732(2)	6980(4)	49(3)
C37	−253(7)	5686(2)	6215(5)	59(3)
C38	531(7)	5509(2)	5732(4)	52(3)
C39	1599(6)	5371(2)	5967(4)	41(3)
C40	1863(7)	5412(2)	6753(4)	38(3)
O7	1824(4)	4880(1)	8083(2)	44(2)
O8	2432(6)	4572(2)	7850(4)	40(3)
C50	1884(6)	4230(2)	7607(4)	38(3)
C51	2643(7)	3948(2)	7357(4)	49(3)
C52	3836(7)	3998(2)	7337(4)	50(3)
C53	4405(6)	4334(2)	7583(3)	39(3)
C54	3654(6)	4626(2)	7857(3)	38(3)
N3	2732(6)	5333(2)	9262(3)	65(3)
N4	3849(6)	5786(2)	8181(4)	59(3)

Co(dafl)(3,6-DBSQ)$_2$. Black crystals of the complex were grown from toluene. Axial photographs indicated monoclinic symmetry and the centered settings of 25 intense reflections with 2θ values between 19 and 34° gave the unit cell dimensions listed in Table 1. Data were collected by θ–2θ scans within the angular range 3.0–50°. Density measurements together with the unit cell volume indicated that there were two complex molecules per unit cell. The coordinates of the cobalt atom were determined using a sharpened Patterson map and phases generated from

(6) (a) Belostotskaya, I. S.; Komissarova, N. L.; Dzhuaryan, E. V.; Ershov, V. V. *Izr. Akad. Nauk, SSSR* **1972**, 1594. (b) Dickeson, J. E.; Summers, L. A. *Aust. J. Chem.* **1970**, *23*, 1023. (c) Henderson, L. J., Jr.; Fronczek, F. R.; Cherry, W. R. *J. Am. Chem. Soc.* **1984**, *106*, 5876.

(7) Jung, O.-S.; Pierpont, C. B. *J. Am. Chem. Soc.* **1994**, *116*, 127.

Table 3. Selected Atom Coordinates (×10⁴) and Equivalent Isotropic Displacement Parameters (Å²) for Co(NO_2phen)(3,6-DBSQ)$_2$

	x/a	*y/b*	*z/c*	*U*(eq)
Co	0	756(1)	0	46(1)
O1	1222(6)	1458(6)	893(4)	53(3)
O2	1200(6)	−554(7)	219(5)	56(4)
C1	2098(9)	834(11)	1120(6)	51(5)
C2	2045(10)	−312(9)	748(7)	52(5)
C3	2963(9)	−1108(10)	964(7)	56(5)
C4	3894(9)	−704(11)	1529(7)	63(5)
C5	3879(9)	418(12)	1877(6)	70(5)
C6	3046(9)	1205(10)	1699(6)	46(5)
O3	−1212(6)	1435(6)	450(4)	55(3)
O4	−1126(6)	−605(7)	−172(5)	64(4)
C15	−2069(9)	806(11)	347(6)	51(4)
C16	−1990(9)	−374(9)	30(6)	47(5)
C17	−2874(10)	−1219(10)	−81(7)	55(5)
C18	−3778(10)	−816(13)	108(7)	78(6)
C19	−3858(10)	334(12)	423(8)	75(6)
C20	−3031(9)	1155(10)	559(7)	48(4)
N1	−15(8)	2523(7)	−475(7)	56(4)
N2	−24(6)	503(8)	−1196(5)	47(4)
C29	−7(8)	2604(11)	−1236(7)	48(5)
C30	21(9)	3746(13)	−1583(10)	73(7)
C31	7(10)	4735(12)	−1122(11)	75(7)
C32	24(10)	4601(12)	−364(10)	80(7)
C33	1(13)	3480(9)	−60(9)	55(4)
C34	1(9)	1480(12)	−1620(9)	60(6)
C35	21(10)	1469(17)	−2369(10)	78(8)
C36	−13(13)	345(28)	−2729(11)	114(12)
C37	−9(12)	−619(16)	−2334(13)	84(9)
C38	−33(8)	−507(10)	−1536(9)	64(6)
C39	43(11)	3610(20)	−2387(10)	86(8)
C40	74(10)	2583(22)	−2765(9)	85(8)
N3	86(13)	4786(22)	−2806(11)	127(10)
O5	224(15)	4713(13)	−3440(9)	191(10)
O6	−222(17)	5672(16)	−2606(12)	188(11)

the location of this atom gave the positions of other atoms of the structure including the locations of two toluene solvent molecules of crystallization. Final cycles of refinement converged with discrepancy indices of R = 0.061 and R_w = 0.061. Selected atom positions are listed in Table 4; tables containing a full listing of atom positions, anisotropic displacement parameters, and hydrogen atom locations are available as supplementary material.

Results

Synthetic procedures have been developed for the formation of a series of bis(quinone) complexes of cobalt that contain a variety of chelating nitrogen-donor coligands. Differences in coligand donation may be used to modulate the orbital energy of the central cobalt atom permiting investigation of the dependence of charge distribution on subtle changes in coligand bonding effects. This would appear as a change in the Co(III)/Co(II) transition temperature (T_c) for the reaction shown in eq 2. Since Co(III) and Co(II) forms of the complexes have

$$Co^{III}(N\text{–}N)(SQ)(Cat) \rightleftarrows Co^{II}(N\text{–}N)(SQ)_2 \qquad (2)$$

characteristic electronic spectra, optical spectroscopy has been used to monitor equilibria in toluene solutions over an appropriate temperature range. This procedure has been used to estimate solution T_c temperatures. The possibility for electron transfer in solid samples of the complexes has also been investigated. The temperature dependence of optical spectra has been used to provide information on the Co(III)/Co(II) transition in the solid state, and the temperature dependence of magnetic properties has also been investigated for selected members of the series. Crystallographic structure determinations have been carried out for three complexes that either have an unusually high T_c value (Co(tmeda)(3,6-DBSQ)(3,6-DBCat)) or remain exclusively in the Co(II) form at all temperatures measured (Co(NO_2phen)(3,6-DBSQ)$_2$, Co(dafl)(3,6-DBSQ)$_2$)).

Table 4. Selected Atom Coordinates (×10⁴) and Equivalent Isotropic Displacement Parameters (Å²) for Co(dafl)(3,6-DBSQ)$_2$

	x/a	*y/b*	*z/c*	*U*(eq)
Co	0	977(1)	0	55(1)
O1	1193(7)	1703(7)	900(4)	63(3)
O2	1200(8)	−328(8)	217(5)	60(4)
C1	2060(11)	1044(11)	1173(6)	49(5)
C2	2052(11)	−119(10)	788(7)	51(5)
C3	2947(11)	−915(11)	1065(7)	54(5)
C4	3807(10)	−538(11)	1656(7)	60(5)
C5	3809(13)	616(11)	1995(7)	66(6)
C6	2957(12)	1380(12)	1781(8)	54(5)
O3	−1199(8)	1688(7)	461(5)	66(4)
O4	−1137(8)	−335(9)	−175(5)	63(4)
C15	−2039(10)	1042(12)	441(6)	53(5)
C16	−1990(11)	−152(11)	78(6)	54(5)
C17	−2858(11)	−971(13)	64(6)	60(5)
C18	−3738(11)	−600(13)	325(8)	75(7)
C19	−3797(13)	552(13)	662(7)	69(6)
C20	−2957(13)	1325(12)	719(7)	58(6)
N1	8(12)	2832(14)	−514(9)	95(7)
N2	12(10)	666(12)	−1391(6)	81(5)
C29	17(13)	2839(18)	−1259(9)	82(7)
C30	46(13)	3805(13)	−1717(10)	79(7)
C31	15(14)	4901(15)	−1382(12)	98(8)
C32	10(14)	4917(17)	−593(13)	100(9)
C33	−16(19)	3884(22)	−213(10)	104(9)
C34	21(11)	1756(13)	−1681(9)	61(6)
C38	20(13)	−205(13)	−1904(13)	91(9)
C37	72(15)	−42(20)	−2650(10)	103(10)
C36	73(13)	1107(14)	−2940(9)	85(7)
C35	49(12)	2032(15)	−2411(9)	74(7)
C39	67(13)	3335(15)	−2482(10)	83(8)
O5	72(10)	3931(9)	−3040(6)	112(6)

Table 5. Electronic Spectra and Solution Co(III)/Co(II) Transition Temperature for the Co(N-N)(3,6-DBQ)$_2$ Series

	Co^{III}(N-N)(3,6-DBSQ)-(3,6-DBCat)		Co^{II}(N-N)-(3,6-DBSQ)$_2$	
N-N	λ_{max}, nm[a]	Cat → Co(III) CT,[b] nm	λ_{max}, nm	T_c,[c] K
$(py)_2CO$	590	2200		>320
tmeda	650, 730 (sh)	2400	850	310
bpy	600, 710 (sh)	2650	820	275
phen	600, 700 (sh)	2550	850	265
dppz	590	2500	850	265
NO_2phen	560		820	<180
dafl			820	≪180

[a] Spectra were recorded in toluene solution. Molar extinction coefficients for the 600-nm transitions of Co^{III}(N-N)(3,6-DBSQ)(3,6-DBCat) and the 850-nm transitions of Co^{II}(N-N)(3,6-DBSQ)$_2$ were in the 1.0 × 10³ to 1.5 × 10³ M^{-1} cm^{-1} range. [b] Recorded for solid samples in a KBr matrix. [c] T_c is defined as the approximate temperature at which concentrations of Co(III) and Co(II) forms of the complexes are equal in toluene solution.

Optical Spectra. Prominent bands that appear in the electronic spectra of members of the Co(N-N)(DBQ)$_2$ series are listed in Table 5. Spectra recorded in toluene solution at temperatures where different tautomeric forms of the complex exist show features that are characteristic of the Co(III) and Co(II) charge distributions, and estimated values of T_c for the complexes included in this investigation are listed in the table. As a general feature, complexes of the Co^{III}(N-N) (DBSQ) (DBCat) charge distribution, where DBQ may be either the 3,5- or 3,6-di-*tert*-butylquinone, show characteristic absorptions in the 600–650-nm range of the visible region. Molar extinction coefficients for this transition are generally close to 1.2 × 10³ M^{-1} cm^{-1}, and the band occasionally shows a shoulder on the low-energy side near 700 nm. Forms of the complexes in the Co^{II}(N–N)(DBSQ)$_2$ charge distribution show characteristic absorptions in the 800–850-nm region, and these bands also have extinction coefficients of approximately 1.2 × 10³ M^{-1} cm^{-1}. Figures 1 and 2 show the temperature-dependent spectral changes in the visible and near-IR regions for Co(bpy)(3,5-DBQ)$_2$ and Co(tmeda)(3,6-DBQ)$_2$.

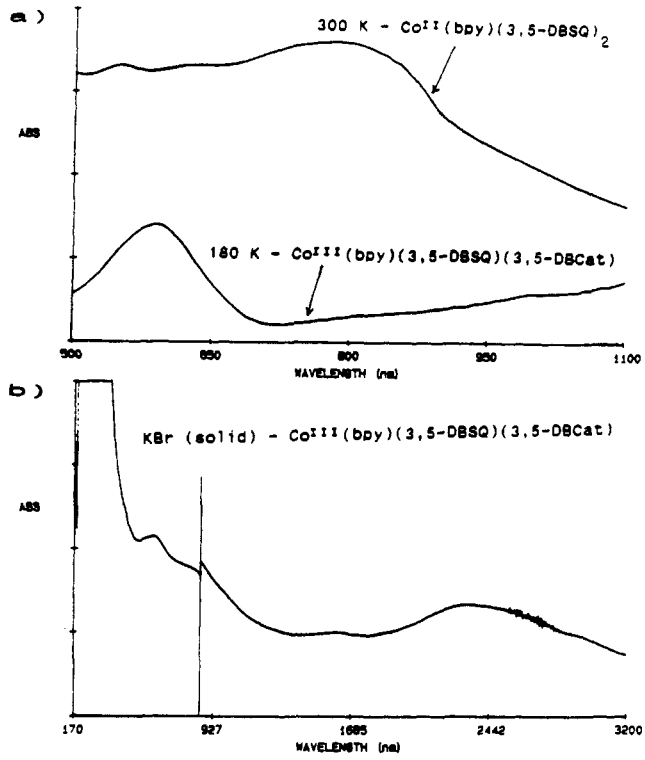

Figure 1. Electronic spectra of Co(bpy)(3,5-DBSQ)(3,5-DBCat): (a) spectra recorded in toluene solution ($C = 2.2 \times 10^{-4}$ M) at temperatures of 180 and 300 K; (b) spectrum recorded on a solid sample at 298 K prepared as a KBr pellet.

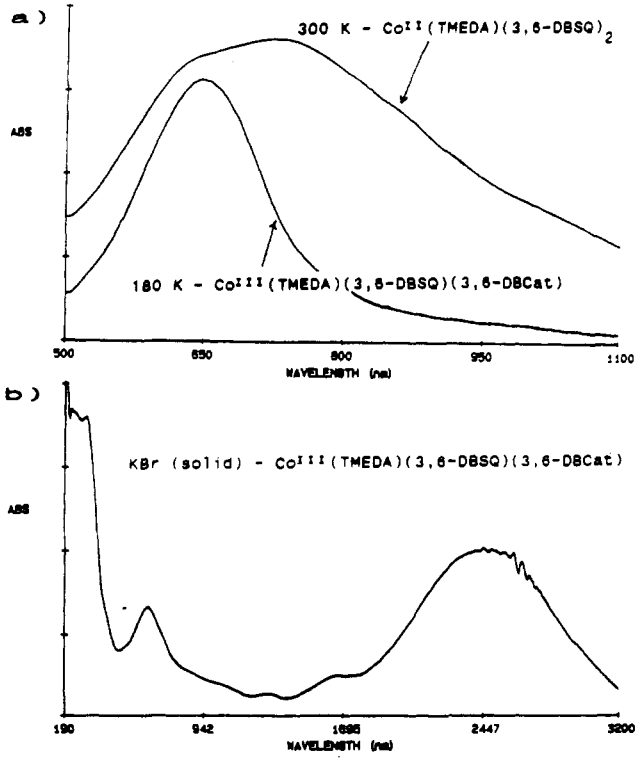

Figure 2. Electronic spectra of Co(tmeda)(3,6-DBSQ)(3,6-DBCat): (a) spectra recorded in toluene solution ($C = 5.9 \times 10^{-4}$ M) at temperatures of 180 and 300 K; (b) spectrum recorded on a solid sample at 298 K prepared as a KBr pellet.

Solutions of the complexes generally change from a dark blue color that is characteristic of the Co(III) charge distribution on the low-temperature side of T_c to a blue-green color of the Co(II) form at higher temperatures. Solution spectra recorded for the complexes at 300 K (Figures 1 and 2) show that at this temperature a mixture of Co(III) and Co(II) species exist at equilibrium.

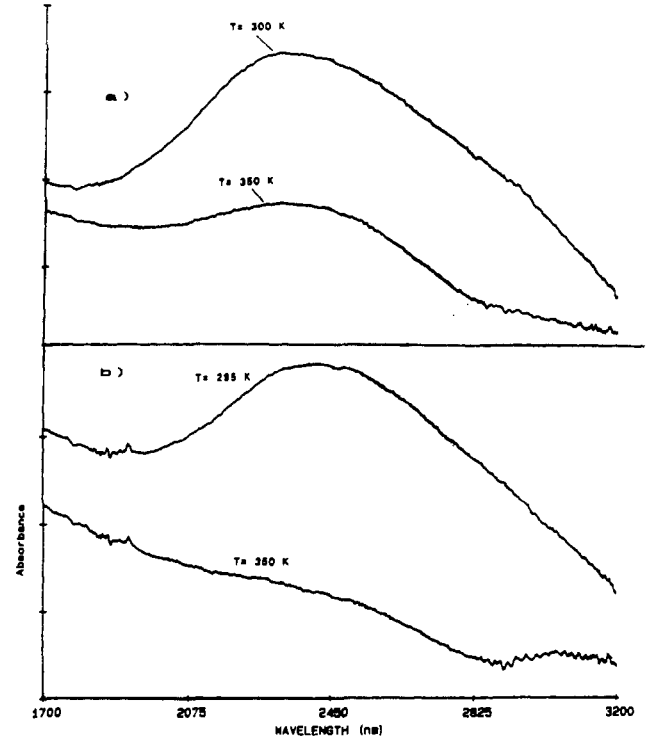

Figure 3. Temperature-dependent changes in the intensity of the Cat → Co(III) charge transfer band of Co(bpy)(3,5-DBSQ)(3,5-DBCat) (a) and Co(phen)(3,6-DBSQ)(3,6-DBCat) (b) recorded on solid samples at temperatures of 300 and 350 K.

Values of T_c given in Table 5 appear to follow a pattern of ligand donor strength, although comparative information on donation is not available for all members of the series. The bis(2-pyridyl) ketone ($(py)_2CO$) coligand gives a complex that remains in the Co(III) charge distribution over the 180–300 K temperature range in toluene solution. This is the only pyridine-based ligand of the series that bonds with a six-membered chelate ring, and donation to Co(III) may be more effective. The diazafluorenone (dafl) coligand gives a complex at the opposite extreme in remaining in the Co(II) form at all temperatures. The coordination properties of this ligand have been found in previous studies to be anomalous, and origins of this effect will be described below with the results of structural characterization on Co(dafl) (3,6-DBSQ)$_2$.

Infrared spectra recorded on solid samples of the complexes included in this investigation often showed intense transitions in the 4000-cm^{-1} region. These bands appear characteristically for the Co^{III}(N-N)(DBSQ)(DBCat) forms and are sometimes more intense than the 600-nm absorption. Spectra recorded for Co^{III}(bpy)(3,5-DBSQ)(3,5-DBCat) and Co^{III}(tmeda)(3,6-DBSQ)(3,6-DBCat) over the 200–3200-nm range for solid samples are shown in Figures 1 and 2. An intense low-energy transition appears prominently in the 2500-nm regions of both compounds. Similar spectra have been recorded for other complexes of the series and the positions of the low-energy transitions are given in Table 5. The bands are broad and sometimes unsymmetrical, but the λ_{max} values follow the T_c values in their correlation with coligand donation. Temperature-dependent changes in optical spectrum may be used to follow shifts in the Co(III)/Co(II) equilibrium that occur in the solid state. Changes in the intensity of the low-energy transitions of Co^{III}(bpy)(3,5-DBSQ)(3,5-DBCat) and Co^{III}(phen)(3,6-DBSQ)(3,6-DBCat) at 300 and 350 K appear in Figure 3. At the higher temperature band intensity indicates the presence of the Co(III) form with the bpy coligand, while with phen the equilibrium has shifted almost entirely to Co^{II}(phen)(3,6-DBSQ)$_2$. Solid-state spectral changes occur reversibly and may be used to obtain T_c values for solid samples. In general, the pattern of values follows the coligand dependence

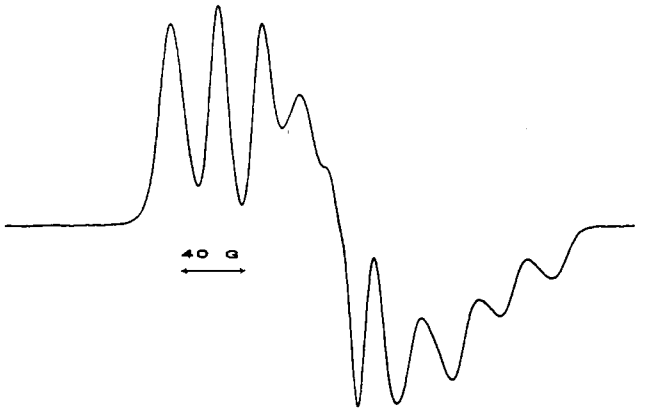

Figure 4. EPR spectrum of Co(tmeda)(3,6-DBSQ)(3,6-DBCat) recorded in a toluene glass at 77 K.

found in solution, but with a shift of approximately 40 °C higher in temperature. Magnetic measurements provide a more convenient means of monitoring the Co(III)/Co(II) transition in the solid state, however.

Magnetism and EPR Spectra. In our initial report on Co(bpy)(3,5-DBSQ)(3,5-DBCat) the Co(III)/Co(II) equilibrium was observed in toluene solution by monitoring changes in magnetism, with accompanying changes in EPR and NMR spectra.[1] More recent reports by Abakumov and Hendrickson have demonstrated that magnetic measurements may be used to examine equilibria occurring in the solid state,[2,3] and in a communication describing the properties of Co(phen)(3,6-DBSQ)(3,6-DBCat) and Co(NO_2phen)(3,6-DBSQ)$_2$, we presented magnetic data that indicated that the phen complex underwent the Co(III)/Co(II) transition, while with NO_2phen, the complex remained in the Co(II) form at all temperatures.[7] Magnetic measurements are an effective means of following the equilibrium due to the change in metal spin state as well as the shift in charge distribution. The Co^{III}(N-N)(DBSQ)(DBCat) species contain low-spin Co(III), with the radical semiquinone ligand as the paramagnetic center of the molecule. As radical-based $S = {}^1/_2$ molecules they show isotropic EPR spectra that are centered near $g = 2.00$, with ^{59}Co ($I = {}^7/_2$) hyperfine coupling that is typically less than 30 G. In toluene glass (77 K) the spectra show slight anisotropy, an effect that is common for delocalized organic radicals.[8] The anisotropic spectrum of Co(tmeda)(3,6-DBSQ)(3,6-DBCat) is shown in Figure 4. It consists of two components, $g_1 = 2.0101$ and $g_2 = 2.0005$, each coupled to the cobalt nucleus with constants of $A_1 = 32$ G and $A_2 = 27$ G.

Electron transfer from the catecholate ligand to the metal of Co^{III}(N-N)(DBSQ)(DBCat) is accompanied by a spin transition of the resulting Co(II) ion. The $S = {}^3/_2$ Co(II) center of the Co^{II}(N-N)(DBSQ)$_2$ product couples with the two $S = {}^1/_2$ radical ligands to give spin states of $S = {}^5/_2$, ${}^3/_2$, and ${}^1/_2$.[3] Metal dπ and dσ electrons may interact differently with the π radical spins and the radical ligands may couple with one another. As a consequence, temperature-dependent magnetic behavior may be complicated, and the use of magnetic data to give a value for T_c in the solid state is tenuous. Further complicating magnetic behavior is the dependence of the spin-transition on solid state effects such as solvation and intermolecular interactions. A single complex may show different behavior depending on the recrystallization procedure.[3] Changes in magnetic moment for Co(bpy)(3,5-DBSQ)(3,5-DBCat) in toluene solution were reported earlier and appeared as a sigmoid plot with moment increasing with temperature.[1] The magnetic moment at 210 K was measured to be 2.35 μ_B; at 330 K the moment was 4.26 μ_B, with the greatest change occurring over a temperature interval of 100° and the

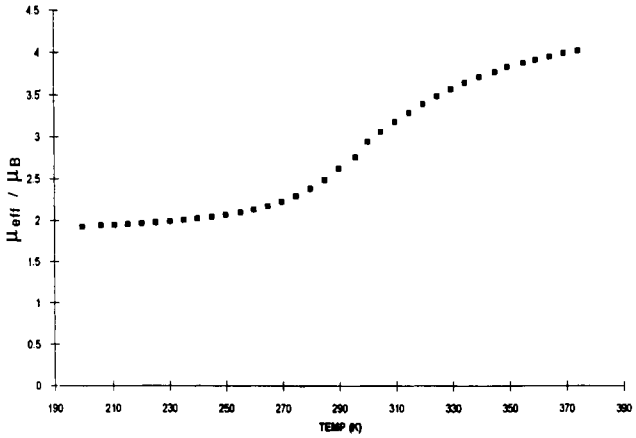

Figure 5. Changes in the magnetic moment of Co(bpy)(3,6-DBSQ)(3,5-DBCat) over the temperature range from 200 to 375 K.

midpoint near 270 K. The results of magnetic measurements recorded on a solid sample of Co(bpy)(3,5-DBSQ)(3,5-DBCat) are shown in Figure 5. At 200 K the magnetic moment is 1.92 μ_B, and there is a small increase to 2.10 μ_B at 260 K. Between 260 and 360 K there is a sharper increase to 3.87 μ_B, and between 360 and 380 K the moment increases further to 4.02 μ_B. The midpoint temperature is approximately 310 K, roughly 40 deg higher than the Co(III)/Co(II) transition temperature estimated in toluene solution from either spectroscopic or magnetic changes. Further, the temperature interval of greatest change in magnetic moment of the solid sample corresponds to the temperature range where the 2300-nm transition shows the greatest decrease in intensity in the solid state. Magnetic measurements have been reported for several complexes of the Co(N-N)(DBQ)$_2$ series. Relatively sharp transitions have been observed for Co(bpy)(3,6-DBSQ)(3,6-DBCat),[2] Co(phen)(3,5-DBSQ)(3,5-DBCat),[3] the pyrazine polymer [Co(pyz)(3,6-DBSQ)(3,6-DBCat)]$_n$,[9] and now Co(bpy)(3,5-DBSQ)(3,5-DBCat). Changes that occur over a relatively broad temperature range have been observed for Co(phen)(3,6-DBSQ)(3,6-DBCat)[7] and Co(bpy)(4-MeO-3,6-DBSQ)(4-MeO-3,6-DBCat).[2] Co(NO_2phen)(3,6-DBSQ)$_2$[7] and Co(Me_2bpy)(3,5-DBSQ)$_2$[3] showed little variation in temperature as complexes of Co(II) over the entire temperature range, and the 2,2′-bipyrazine complex Co(bpyz)(3,5-DBSQ)(3,5-DBCat)[3] remained in the Co(III) form. Differences in the limiting magnetic moments at high temperature for Co(II) complexes result from the spin-coupling effects described earlier. Values range from the 380 K moment of 4.02 μ_B for Co(bpy)(3,5-DBSQ)$_2$ to a value of 6.04 μ_B at 340 K for Co(phen)(3,6-DBSQ)$_2$.[7] The lower value is slightly greater than the $S = {}^3/_2$ moment that would result from strong antiparallel coupling between the single unpaired dπ electron and one of the π_{SQ} spins, and the larger values are close to the $S = {}^5/_2$ moment resulting from parallel spin alignment. Crystallographic characterization on various members of the series has shown that in cases where planar nitrogen-donor coligands are used, strong intermolecular stacking interactions occur,[1-3] and intermolecular contributions to the magnetic properties may also be significant.

Structural Features of the Co(N-N)(DBQ)$_2$ Complexes. Our earlier structural characterization on Co(bpy)(3,5-DBSQ)(3,5-DBCat) gave Co–O and Co–N lengths that were more typical of low spin Co(III) than high-spin Co(II). This structure determination was carried out at ambient room temperature, and with the insights provided by the magnetic data and infrared spectroscopy described herein, we now know that a fraction of the molecules present in the solid-state lattice are in the high-spin Co(II) form. Rheingold and Hendrickson have demonstrated the structural changes associated with the Co(III)/Co(II)

(8) For example: Bresgunov, A. Y.; Dubinsky, A. A.; Poluektov, O. G.; Lebedev, Y. S.; Prokof'ev, A. I. *Mol. Phys.* **1992**, *75*, 1123.

(9) Jung, O.-S.; Pierpont, C. G. *J. Am. Chem. Soc.* **1994**, *116*, 2229.

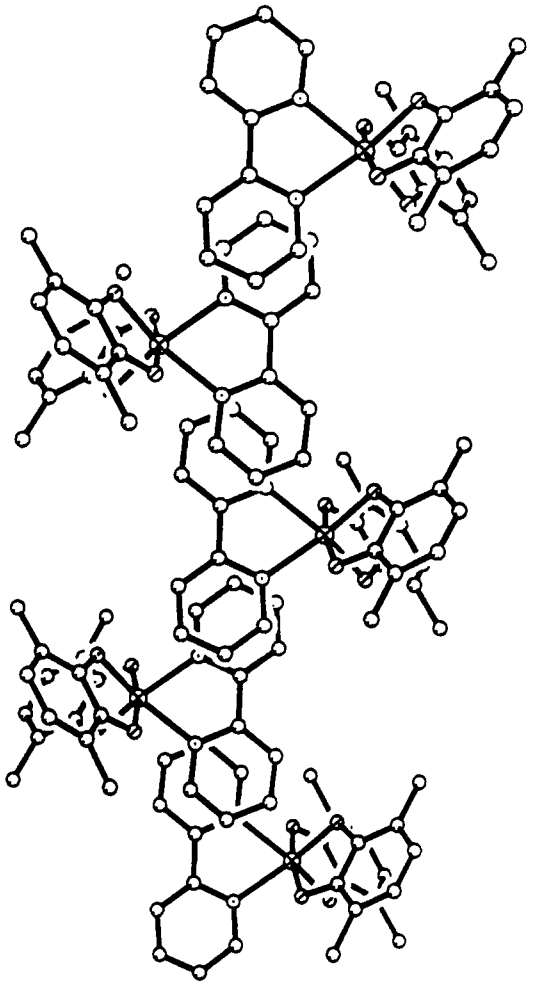

Figure 6. Intermolecular stacking between bipyridine ligands of Co(bpy)(3,6-DBSQ)(3,6-DBCat).

transition by carrying out structure determinations on Co(phen)(3,5-DBQ)$_2$ at high (295 K), intermediate (283 K), and low (173 K) temperatures to follow the changes in bond length accompanying the transition.[3] Changes in molecular volume produced by light-induced Co(III)/Co(II) transitions are responsible for photomechanical "crystal bending" effects for the [Co(pyz)(3,6-DBSQ)(3,6-DBCat)]$_n$ polymer[9] and Co(bpy)(3,6-DBSQ)(3,6-DBCat).[2] The mechanical effects result from macroscopic changes in axial length produced by individual changes in molecular volume propagated along the chain length of an extended one-dimensional lattice. A view of the Co(bpy)(3,6-DBSQ)(3,6-DBCat) lattice formed by stacked bpy ligands of adjacent molecules is shown in Figure 6.

Co(tmeda)(3,6-DBSQ)(3,6-DBCat). Spectral characterization on solid samples of Co(tmeda)(3,6-DBSQ)(3,6-DBCat) indicate that it has one of the highest T_c values of the series of compounds included in this study. As a complex that is representative of one extreme in the series, it has been characterized crystallographically, and a view of one molecule is shown in Figure 7. There are two independent complex molecules in the asymmetric region of the monoclinic unit cell and the features of the two molecules are within error of being identical. Averaged bond lengths and angles are listed in Table 6. In the figure, oxygen atoms O1 and O2 are associated with the semiquinone ligand, O3 and O4 belong to the catecholate. This is apparent from the ligand C–O lengths which average to 1.305(8) Å for the semiquinone and 1.344(8) Å for the catecholate ligands of the two molecules. Further, the C_3–C_4 and C_5–C_6 bonds of the semiquinone ligands are slightly contracted (1.367(8) Å) relative to the aromatic values of the catecholate ring C–C bonds, and the SQ C_1–C_2 lengths (1.433(8) Å) are slightly longer than the

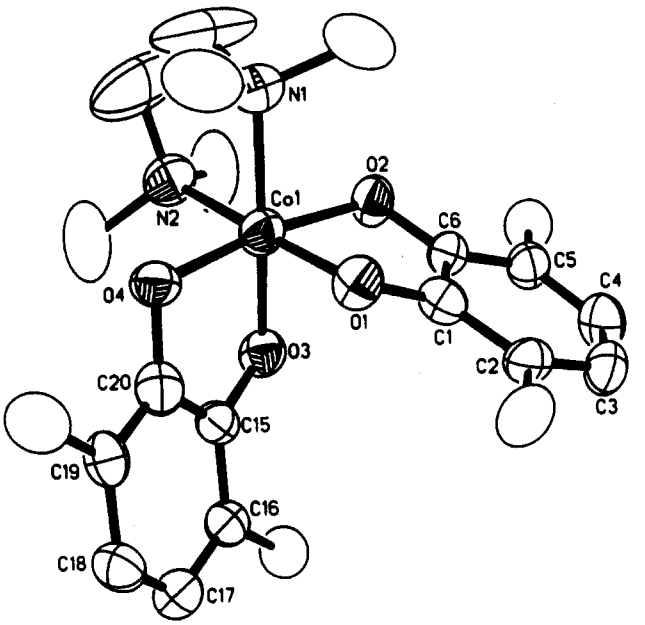

Figure 7. View of Co(tmeda)(3,6-DBSQ)(3,6-DBCat) with methyl carbon atoms of the *tert*-butyl groups omitted. Oxygen atoms O1 and O2 are bound to the semiquinone ligand; O3 and O4 are bound to the catecholate.

Table 6. Selected Average Bond Lengths and Angles for Co(tmeda)(3,6-DBSQ)(3,6-DBCat)[a]

	Bond Lengths (Å)		
	Cobalt		
Co1–O1	1.864(4)	Co1–O4	1.873(4)
Co1–O2	1.899(4)	Co1–N1	2.031(6)
Co1–O3	1.852(4)	Co1–N2	2.021(6)
	Semiquinone		
O1–C1	1.304(8)	C3–C4	1.396(9)
O2–C6	1.306(8)	C4–C5	1.372(9)
C1–C2	1.420(9)	C5–C6	1.411(9)
C2–C3	1.364(9)	C1–C6	1.433(9)
	Catecholate		
O3–C15	1.342(8)	C17–C18	1.376(9)
O4–C20	1.345(8)	C18–C19	1.401(9)
C15–C16	1.400(9)	C19–C20	1.401(9)
C16–C17	1.388(9)	C15–C20	1.401(9)
	Bond Angles (deg)		
	Cobalt		
O1–Co1–O2	85.2(2)	O2–Co1–N2	93.8(2)
O1–Co1–O3	89.9(2)	O3–Co1–O4	87.0(2)
O1–Co1–O4	88.1(2)	O3–Co1–N1	177.8(2)
O1–Co1–N1	92.2(2)	O3–Co1–N2	90.8(2)
O1–Co1–N2	179.0(2)	O4–Co1–N1	93.6(2)
O2–Co1–O3	87.9(2)	O4–Co1–N2	92.7(2)
O2–Co1–O4	171.8(2)	N1–Co1–N2	87.1(3)
O2–Co1–N1	91.9(2)		
	Semiquinone		
Co1–O1–C1	110.1(4)	O1–C1–C6	115.7(6)
Co1–O2–C6	109.0(4)	O2–C6–C1	115.3(6)
	Catecholate		
Co1–O3–C15	109.0(4)	O3–C15–C20	115.2(6)
Co1–O4–C20	107.5(4)	O4–C20–C15	116.0(6)

[a] The atom numbering scheme follows the labeling in Figure 7 with O1 and O2 associated with the semiquinone ligand and O3 and O4 with the catecholate. Corresponding values have been for the two crystallographically independent molecules.

aromatic value. These features have been found to occur characteristically for semiquinone ligands. Each of the Co–O lengths in the two molecules is unique. The shortest are the Co–O_{Cat} lengths *trans* to the tmeda nitrogen atoms with an average length of 1.852(4) Å, the longest are the Co–O_{SQ} lengths *trans*

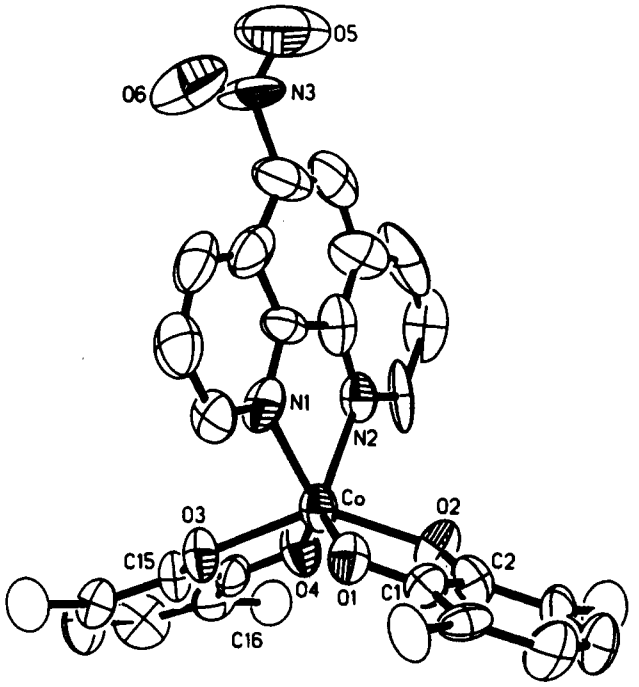

Figure 8. View of $Co(NO_2phen)(3,6\text{-}DBSQ)_2$. The complex molecule is trigonal prismatic with a twist angle of 3.7°.

Table 7. Selected Bond Lengths and Angles for $Co(dafl)(3,6\text{-}DBSQ)_2$

	Bond Lengths (Å)		
	Cobalt		
Co–O1	2.043(7)	Co–O4	2.005(10)
Co–O2	2.050(9)	Co–N1	2.278(16)
Co–O3	2.043(10)	Co–N2	2.518(16)
	Semiquinone 1		
O1–C1	1.289(14)	C3–C4	1.354(16)
O2–C2	1.280(14)	C4–C5	1.430(18)
C1–C2	1.475(17)	C5–C6	1.336(20)
C2–C3	1.408(17)	C1–C6	1.384(16)
	Semiquinone 2		
O3–C15	1.260(16)	C17–C18	1.360(2)
O4–C16	1.273(17)	C18–C19	1.437(21)
C15–C16	1.498(18)	C19–C20	1.339(21)
C16–C17	1.410(19)	C15–C20	1.393(22)
	Bond Angles (deg)		
	Cobalt		
O1–Co–O2	78.5(3)	O2–Co–N2	83.9(4)
O1–Co–O3	88.7(3)	O3–Co–O4	78.1(4)
O1–Co–O4	138.3(3)	O3–Co–N1	83.5(5)
O1–Co–N1	82.7(4)	O3–Co–N2	130.5(4)
O1–Co–N2	129.9(4)	O4–Co–N1	133.4(4)
O2–Co–O3	140.4(3)	O4–Co–N2	86.1(4)
O2–Co–O4	87.0(4)	N1–Co–N2	74.1(5)
O2–Co–N1	130.5(5)		
	Semiquinone 1		
Co–O1–C1	115.2(7)	O1–C1–C2	115.4(9)
Co–O2–C2	115.0(8)	O2–C2–C1	115.9(10)
	Semiquinone 2		
Co–O3–C15	116.5(8)	O3–C15–C16	113.6(12)
Co–O4–C16	116.2(8)	O4–C16–C15	115.6(11)

with catecholate oxygen atoms (1.899(4) Å), and the $Co–O_{Cat}$ lengths are approximately 0.14 Å shorter than corresponding semiquinone bond lengths. Co–N lengths of the tmeda ligands show the effects of the difference in *trans* influence between SQ and Cat ligands with an average Co–N value of 2.021(6) Å for nitrogens opposite SQ oxygen atoms and a value of 2.031(6) Å at positions *trans* to Cat oxygen atoms.

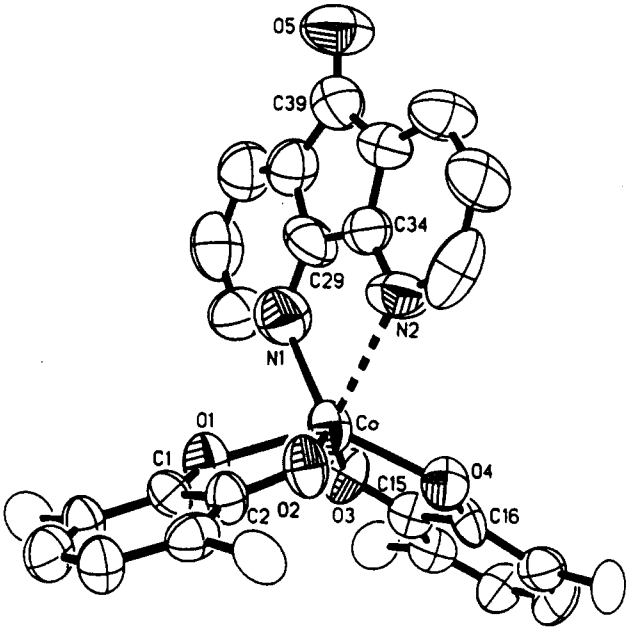

Figure 9. View of $Co(dafl)(3,6\text{-}DBSQ)_2$. The complex molecule is trigonal prismatic with a twist angle of 4.2°.

The localized charge distribution of the complex is clear from the distinction between SQ and Cat ligands and the bond lengths to the metal. Lengths to high-spin Co(II) would be roughly 0.20 Å longer than those found in this structure determination.

$Co(NO_2phen)(3,6\text{-}DBSQ)_2$. The spectroscopy on toluene solutions of the nitrophenanthroline complex was markedly different from the temperature dependent behavior of the phen complex. At 300 K a strong transition at 820 nm was observed that is characteristic of the Co(II) charge distribution. This spectrum persisted to 180 K where a new transition at 560 nm appeared that is characteristic of the Co(III) form. The Co(III)/Co(II) T_c for $Co(NO_2phen)(3,6\text{-}DBSQ)_2$ lies below 180 K, but it is possible to see evidence for the formation of $Co(NO_2phen)(3,6\text{-}DBSQ)(3,6\text{-}DBCat)$ in solution at 180 K. Spectra recorded on solid samples of the complex failed to indicate the presence of the Co(III) form under normal conditions of spectral resolution. Crystals were obtained from a toluene solution and used for a structure determination. A view of the complex molecule is shown in Figure 8, with bond lengths and angles listed in Table 7. As shown in the figure, the molecule is trigonal prismatic in structure with a twist angle of 3.7°. Lengths of the Co–O bonds are 0.20 Å longer than values of Co(tmeda)(3,6-DBSQ)(3,6-DBCat), and the Co–N lengths are 0.15 Å longer for $Co(NO_2phen)(3,6\text{-}DBSQ)(3,6\text{-}DBCat)$. Semiquinone C–O lengths average 1.27(1) Å, while the pattern of C–O lengths for the tmeda complex is consistent with the localized SQ–Cat charge distribution. Ligand field effects allow a trigonal prismatic geometry for high-spin Co(II), and a few examples have been characterized structurally.[10] Low-spin Co(III) would be expected to be rigidly octahedral.[11]

$Co(dafl)(3,6\text{-}DBSQ)_2$. Spectral features of the diazafluorenone complex in toluene solution are similar to those of the complex prepared with nitrophenanthroline. A transition appears at 820 nm for the complex at room temperature, and there is no evidence for a low-energy transition in the 2500-nm region in the solid-state spectrum at room temperature. It differs from the NO_2-phen complex in failing to indicate the appearance of a Co(III) form at 180 K. Crystallographic characterization of $Co(dafl)(3,6\text{-}DBSQ)_2$ has shown that the molecule is also trigonal prismatic

(10) (a) Bertrand, J. A.; Kelly, J. A.; Vassian, E. G. *J. Am. Chem. Soc.* **1969**, *91*, 2394. (b) Larsen, E.; La Mar, G. N.; Wagner, B. E.; Parks, J. E.; Holm, R. H. *Inorg. Chem.* **1972**, *11*, 2652.

(11) Kepert, D. L. *Prog. Inorg. Chem.* **1977**, *23*, 1.

Table 8. Selected Bond Lengths and Angles for $Co(NO_2phen)(3,6\text{-}DBSQ)_2$

	Bond Lengths (Å)		
	Cobalt		
Co–O1	2.063(6)	Co–O4	2.060(6)
Co–O2	2.078(6)	Co–N1	2.169(7)
Co–O3	2.061(6)	Co–N2	2.161(7)
	Semiquinone 1		
O1–C1	1.282(9)	C3–C4	1.364(14)
O2–C2	1.255(9)	C4–C5	1.415(15)
C1–C2	1.451(14)	C5–C6	1.349(15)
C2–C3	1.435(14)	C1–C6	1.422(14)
	Semiquinone 2		
O3–C15	1.266(14)	C17–C18	1.354(15)
O4–C16	1.266(14)	C18–C19	1.432(15)
C15–C16	1.463(14)	C19–C20	1.369(15)
C16–C17	1.441(14)	C15–C20	1.423(15)
	Bond Angles (deg)		
	Cobalt		
O1–Co–O2	76.8(3)	O2–Co–N2	84.8(3)
O1–Co–O3	91.8(3)	O3–Co–O4	77.4(3)
O1–Co–O4	138.2(3)	O3–Co–N1	83.3(4)
O1–Co–N1	83.0(3)	O3–Co–N2	128.8(3)
O1–Co–N2	129.3(3)	O4–Co–N1	134.0(3)
O2–Co–O3	140.4(3)	O4–Co–N2	85.8(3)
O2–Co–O4	86.3(3)	N1–Co–N2	74.6(4)
O2–Co–N1	131.2(4)		
	Semiquinone 1		
Co–O1–C1	116.0(6)	O1–C1–C2	114.5(9)
Co–O2–C2	114.7(7)	O2–C2–C1	117.9(10)
	Semiquinone 2		
Co–O3–C15	115.4(7)	O3–C15–C16	115.1(10)
Co–O4–C16	114.6(7)	O4–C16–C15	116.9(10)

in structure (Figure 9). The listing of bond distances and angles given in Table 8 shows that the Co–O and Co–N lengths are consistent with Co(II), with surprising asymmetry in the two Co–N lengths to the dafl ligand. The longer Co–N2 length is 2.518(16) Å, while the Co–N1 length is 2.278(16) Å. A similar pattern was found for $Cu(dafl)_2Cl_2$ with Cu–N values of 1.978(4) and 2.773(4) Å, and unsymmetrical coordination of this type may appear as a general feature of complexes prepared with this ligand.[12]

Structural studies have now been reported for several members of the $Co(N\text{-}N)(DBQ)_2$ series. These complexes range from molecules with relatively high T_c values that are almost entirely in the Co(III) form at the temperature of the structure determination to the NO_2phen and dafl complexes, as molecules that are essentially locked in the Co(II) form in the solid state by their stereochemistry. Changes in metal and ligand bond lengths associated with the shift in charge distribution are summarized in Table 9.

Valence Tautomeric Transformations for the $Co(N\text{-}N)(DBQ)_2$ Series. In an initial report we described the equilibrium shown in eq 1, relating Co(III) and Co(II) forms of Co(bpy)(3,5-DBSQ)(3,5-DBCat).[1] With the change in metal ion spin state that accompanies electron transfer, the equilibrium can be described by equations that separate electron transfer (ET) (eq. 3) and spin transition (ST) (eq 4). Orbitals of $d\pi$ and $d\sigma$ symmetry are, ostensibly, the t_{2g} and e_g levels in regular octahedral symmetry. Spectral characterization on the Co(III) complexes of the series showed that an intense transition in the 2500-nm region of the

$$\underset{(d\pi)^6(d\sigma)^0(\pi_{Q1})^2(\pi_{Q2})^1}{Co^{III}(N\text{-}N)(SQ)(Cat)} \rightleftarrows \underset{(d\pi)^6(d\sigma)^1(\pi_{Q1})^1(\pi_{Q2})^1}{Co^{II}(N\text{-}N)(SQ)_2} \quad (3)$$

$$\underset{(d\pi)^6(d\sigma)^1(\pi_{Q1})^1(\pi_{Q2})^1}{Co^{II}(N\text{-}N)(SQ)_2} \rightleftarrows \underset{(d\pi)^5(d\sigma)^2(\pi_{Q1})^1(\pi_{Q2})^1}{CO^{II}(N\text{-}N)(SQ)_2} \quad (4)$$

infrared appeared characteristically for complexes of this charge distribution. We tentatively assign this band as the Cat → Co(III) charge transfer transition that is associated with the electron transfer step. Photomechanical experiments carried out on both Co(bpy)(3,6-DBSQ)(3,6-DBCat) and $[Co(pyz)(3,6\text{-}DBSQ)(3,6\text{-}DBCat)]_n$ show greatest response to light above 1500 nm in wavelength,[2,9] and the preliminary results of PES experiments carried out to observe light-induced changes in cobalt spin state show the appearance of Co(II) species upon irradiation.[13] As an alternative assignment, the low-energy transitions may result from intervalence transfer between the mixed-charge SQ and Cat ligands. However, complexes of the Fe(N–N)(3,6-DBSQ)(3,6-DBCat)[14] and Ga(N-N)(3,6-DBSQ)(3,6-DBCat)[15] series fail to show bands in this region. Members of the Mn(N-N)(3,6-DBSQ)(3,6-DBCat) series also show low-energy transitions near 2100 nm and exhibit tautomeric equilibria, and there is the appearance of a link between low-energy transitions and valence isomerism.[4a,16] With the Cat → Co(III) assignment for the 2500-nm transitions for members of the $Co^{III}(N\text{-}N)(DBSQ)(DBCat)$ series, two properties of the transition are important. The intensity indicates that spin multiplicity is conserved, in accord with the transient formation of low-spin Co(II) as the product of vertical electron transfer. Secondly, the thermal barrier to electron transfer would be considerably lower in energy, well into the infrared region, partially accounting for the thermal accessibility of forms of the complex differing in charge distribution. The low energy of this electron transfer process results from the ligand field environment created by the quinone and coligands, and differences in coligand donation are responsible for variations in T_c. Not all Co(III)–catecholate complexes have low-energy transitions in the 2500-nm region. Members of the $[Co^{III}(N\text{-}N)_2(3,5\text{-}DBCat)]^+$ (N-N = en, bpy, phen) series[17] show optical transitions of lowest energy in the visible and they fail to exhibit tautomeric equilibria. A critical balance of cobalt and quinone orbital energies is necessary for the electron transfer step. Changes in spin and orbital degeneracy are probably small, the entropic change associated with electron transfer is small, and the energy change associated with the electron transfer step is primarily enthalpic.

Once in the transient low-spin Co(II) form, the spin transition step (ST) (eq 4) becomes important. Reviews on spin transition complexes discuss the entropy increase associated with the increase in spin multiplicity and its effect on spin transition temperature.[18] Subtle solid-state effects that have been described for spin transition complexes seem to carry over to the sample-dependent magnetic properties of the $Co(N\text{-}N)(DBQ)_2$ series. A change of approximately 0.1 Å in metal ion radius is associated with the LS Co(II)/HS Co(II) transition, so much of the structural distortion associated with the equilibrium occurs during the spin transition step.[18a,19]

Thermodynamic changes associated with the combined reaction (eq 2) include contributions from the ET and ST steps.

Table 9. Bond Lengths (Å) for Members of the $Co^{III}(N\text{-}N)(SQ)(Cat)/Co^{II}(N\text{-}N)(SQ)_2$ Series

complex	Co–O	Co–N	$C\text{–}O_{SQ}$	$C\text{–}O_{Cat}$	ref
Co(tmeda)(3,6-DBSQ)(3,6-DBCat)	1.852(4)–1.899(4)	2.021(6)–2.031(6)	1.305(8)	1.344(8)	this work
Co(bpy)(3,5-DBSQ)(3,5-DBCat)	1.851(6)–1.906(6)	1.940(7)–1.957(7)	1.297(9)	1.358(10	1
Co(bpy)(3,6-DBSQ)(3,6-DBCat)	1.912–1.923	1.991	1.311		2
$Co(phen)(3,6\text{-}DBSQ)_2$	1.984(4)–2.011(4)	2.085	1.293(8), 1.304(7)		3
$Co(bpz)(3,5\text{-}DBSQ)_2$	2.046(4)–2.057(4)	2.130(4)	–		3
$Co(NO_2\text{-}phen)(3,6\text{-}DBSQ)_2$	2.066(6)	2.165(7)	1.267(9)		this work
$Co(dafl)(3,6\text{-}DBSQ)_2$	2.005(10)–2.050(9)	2.278(16)–2.518(16)	1.28(1)		this work

$$\Delta G = \Delta G^{ET} + \Delta G^{ST}$$

$$\Delta H = \Delta H^{ET} + \Delta H^{ST}$$

$$\Delta S = \Delta S^{ET} + \Delta S^{ST}$$

At T_c, $\Delta G = 0$, and, for T_c to be positive, ΔH and ΔS must both have same sign.

$$\Delta G = \Delta G^{ET} + \Delta G^{ST} = 0$$

$$T_c = \Delta H/\Delta S = (\Delta H^{ET} + \Delta H^{ST})/(\Delta S^{ET} + \Delta S^{ST})$$

It is unlikely that both ΔG^{ET} and ΔG^{ST} would be zero at the same temperature, and free energy changes for the two steps must be equal in magnitude and opposite in sign at T_c. From the relationship above, it is clear that enthalpy and entropy changes for both the electron transfer and spin transition steps define the condition required for the tautomeric equilibrium. If the entropy change associated with electron transfer is small, and ΔS is approximately equal to ΔS^{ST}, then T_c is strongly dependent upon the effects governing the spin transition, and many of the anomalies associated with spin transition complexes appear for the tautomeric equilibrium. Spin transition is not an intrinsic property of complexes that show valence isomerism, however. Metal ions of the manganese series (eq 5) remain in the high-spin form, but

$$Mn^{IV}(N\text{-}N)(DBCat)_2 \rightleftarrows Mn^{III}(N\text{-}N)(DBSQ)(DBCat)$$

$$Mn^{III}(N\text{-}N)(DBSQ)(DBCat) \rightleftarrows Mn^{II}(N\text{-}N)(DBSQ)_2 \quad (5)$$

here again, there is a large increase in spin degeneracy associated with shifts in charge distribution to provide a significant positive entropic effect.[16] Energy changes associated with equilibria of the related manganese and iron complexes will be described in subsequent publications.

Acknowledgment. We would like to thank Christopher Lange for recording the EPR spectrum on Co(tmeda)(3,6-DBSQ)(3,6-DBCat) and Brenda Conklin for magnetic susceptibility measurements. Support for this research was provided by the National Science Foundation through Grant CHE 90–23636; EPR instrumentation was purchased with NSF Grant CHE 90–21122.

Supplementary Material Available: Tables providing details of synthetic procedures, crystal data and details of the structure determinations, atomic coordinates, anisotropic thermal parameters, hydrogen atom locations, bond lengths, and bond angles for Co(tmeda)(3,6-DBSQ)(3,6-DBCat) and Co(dafl)(3,6-DBSQ)$_2$ (33 pages). Ordering information is given on any current masthead page.

(12) Balagopalakrishna, C.; Rajasekharan, M. V.; Bott, S.; Atwood, J. L.; Ramakrishna, B. L. *Inorg. Chem.* **1992**, *31*, 2843.
(13) Research in progress.
(14) Attia, A.; Pierpont, C. G. *Inorg. Chem.*, submitted for publication.
(15) Lange, C. W.; Conklin, B. J.; Pierpont, C. G. *Inorg. Chem.* **1994**, *33*, 1276.
(16) Attia, A. S.; Pierpont, C. G. *J. Am. Chem. Soc.*, submitted for publication.
(17) (a) Wicklund, P. A.; Brown, D. G. *Inorg. Chem.* **1976**, *15*, 396. (b) Kessel, S. L.; Emberson, R. M.; DeBrunner, P. G.; Hendrickson, D. N. *Inorg. Chem.* **1980**, *19*, 1170. (c) Hartl, F.; Vlcek, A., Jr. *Inorg. Chim. Acta* **1986**, *118*, 57. (d) Bianchini, C.; Masi, D.; Mealli, C.; Meli, A.; Martini, G.; Laschi, F.; Zanello, P. *Inorg. Chem.* **1987**, *26*, 3683. (e) Benelli, C.; Dei, A.; Gatteschi, D.; Pardi, L. *Inorg. Chim. Acta* **1989**, *163*, 99. (f) Jones, M.; Pierpont, C. G. Research in progress.
(18) (a) Gutlich, P. *Struct. Bonding (Berlin)* **1981**, *44*, 83. (b) Konig, E. *Prog. Inorg. Chem.* **1987**, *35*, 527.
(19) Konig, E.; Ritter, G.; Dengler, J.; Thuery, P.; Zarembowitch, J. *Inorg. Chem.* **1989**, *28*, 1757.